HHS Public Access

Author manuscript

Mol Immunol. Author manuscript; available in PMC 2020 August 01.

Published in final edited form as:

Mol Immunol. 2019 August ; 112: 206–214. doi:10.1016/j.molimm.2019.06.001.

Inducible overexpression of zebrafish *microRNA-722* suppresses chemotaxis of human neutrophil like cells

Alan Y. Hsu[1], **Sheng Liu**[2,3], **Ramizah Syahirah**[1], **Kent A. Brasseale**[1], **Jun Wan**[2,3,4], **Qing Deng**[1,5,6,*]

[1.] Department of Biological Sciences, Purdue University, West Lafayette, IN 47907 USA

[2.] Department of Medical and Molecular Genetics, Indiana University School of Medicine, Indianapolis, IN 46202 USA

[3.] Collaborative Core for Cancer Bioinformatics, Indiana University Simon Cancer Center, Indianapolis, IN 46202 USA

[4.] Center for Computational Biology and Bioinformatics, Indiana University School of Medicine, Indianapolis, IN 46202 USA

[5.] Purdue Institute for Inflammation, Immunology, & Infectious Disease, Purdue University, West Lafayette, IN 47907 USA

[6.] Purdue University Center for Cancer Research, Purdue University, West Lafayette, IN 47907 USA

Abstract

Neutrophil migration is essential for battling against infections but also drives chronic inflammation. Since primary neutrophils are terminally differentiated and not genetically tractable, leukemia cells such as HL-60 are differentiated into neutrophil-like cells to study mechanisms underlying neutrophil migration. However, constitutive overexpression or inhibition in this cell line does not allow the characterization of the genes that affect the differentiation process. Here we apply the tet-on system to induce the expression of a zebrafish microRNA, *dre-miR-722,* in differentiated HL-60. Overexpression of *miR-722* reduced the mRNA level of genes in the chemotaxis and inflammation pathways, including *Ras-Related C3 Botulinum Toxin Substrate 2* (RAC2). Consistently, polarization of the actin cytoskeleton, cell migration and generation of the

[*] Corresponding author: G231 Biological Sciences, Purdue University, 915 W. State Street, West Lafayette, IN 47907, Tel: 765-494-0423, Fax: 765-494-0876, qingdeng@purdue.edu.

Authorship: AH, JW and DQ designed research and wrote the manuscript. AH performed the experiments. AH, JW, RS, KB and SL analyzed the data. All authors read and approved the manuscript.

Conflict of interest statement: The authors declare no competing interests.

Data availability statement:

The RNA-seq raw data and processed data deposited to Gene Expression Omnibus (GEO) GSE126527 (https://www.ncbi.nlm.nih.gov/geo/query/acc.cgi?acc=GSE126527). Plasmids are available on Addgene: pCDNA miR-722-Dendra (#97163), pcDNA3.1 Dendra2 (#103967), pSi-check2-hRac2 3'UTR (#97160), pSi-check2-hRac2 - mut 3'UTR (#97161), plix4.03-miR-722 (#97140), plix4.03-vector (#97141).

reactive oxygen species are significantly inhibited upon induced *miR-722* overexpression. Together, zebrafish *miR-722* is a suppressor for migration and signaling in human neutrophil like cells.

Keywords

HL-60; microRNA; chemotaxis; RAC2; signaling; inducible expression

1. Introduction

The neutrophil is the most abundant white blood cell in the circulation and a significant regulator of inflammation. While essential for battling against pathogens, neutrophil activation drives immunopathology in numerous human diseases, including organ transplantation, sepsis, rheumatoid arthritis, diabetes, neurodegenerative disease and cancer (Borregaard, 2010; Nathan, 2006; Soehnlein et al., 2017), although the link of some diseases to the innate immune system is not intuitive. Besides killing pathogens, they communicate with other cells to shape the inflammatory response. For example, neutrophils initiate inflammation by scanning platelets (Sreeramkumar et al., 2014), migrating away from the initial activation site to disseminate inflammation to the lung (Woodfin et al., 2011), priming macrophages by providing DNA in the forms of extracellular traps (Warnatsch et al., 2015) and can directly present antigens to activate T cells (Abi Abdallah et al., 2011; Lim et al., 2015).

Manipulating neutrophil migration and activation is implicated in managing chronic inflammation (Kolaczkowska and Kubes, 2013; Soehnlein et al., 2017). The current challenge in the field is that primary neutrophils are terminally differentiated with a very short life span ex vivo, which excludes the feasibility of genetic manipulation for functional characterization. To model neutrophils, human promyelocytic leukemia HL-60 cells (Pedruzzi et al., 2002) and NB4 cells (Lanotte et al., 1991) are differentiated in culture for 5–7 days into neutrophils-like cells. Gene transduction approaches using either the lenti- or retro-virus are successful in these cell lines, providing a genetically tractable system. However, due to the cell differentiation process, extensive characterization is required to separate the effect of the target genes on cell differentiation and mature cell function. Inducible expression using tet-on (gene expression activated by doxycycline) is widely applied in cancer research and other cell lines. However this technique has not been applied to neutrophil precursor cells.

MicroRNAs (MiRNA) are evolutionarily conserved, non-coding RNAs of ~22 nucleotides that post-transcriptionally regulate gene expression (Fabian and Sonenberg, 2012). miRNAs are master regulators that can simultaneously suppress hundreds of genes and regulate numerous cellular processes and human diseases. miRNA profiles are distinct in human peripheral blood neutrophils (Gantier, 2013; Landgraf et al., 2007; Ward et al., 2011) and activated tissue infiltrating neutrophils (Larsen et al., 2013), suggesting that they are regulated by the inflammation process or tissue environment. On the other hand, only a few miRNAs are functionally characterized in neutrophils (Gurol et al., 2016). In HL-60 cells,

miRNA expression changes during cell differentiation (Jian et al., 2011; Kasashima et al., 2004; Pizzimenti et al., 2009) and after radiation (Liamina et al., 2017) or resveratrol treatment (Ergin et al., 2015). Indeed, multiple miRNAs regulate HL-60 growth, differentiation and survival in vitro (Bousquet et al., 2008; Chen et al., 2010; Huang et al., 2015; Jian et al., 2011; Kawasaki and Taira, 2004; Lin et al., 2015; Sharifi et al., 2014; Shen et al., 2016; S. L. Wang et al., 2016; X. S. Wang et al., 2012). On the other hand, reports on how miRNAs regulate differentiated cell function such as migration is scarce. Introduction of synthetic *miR-155* and *miR-34* mimics into differentiated HL-60 suppressed cell migration but not differentiation (Cao et al., 2017), whereas depleting *miR-155,* on the other hand, induced cell differentiation and apoptosis (Liang et al., 2017).

In zebrafish, we have identified a miRNA, *miR-722,* that when overexpressed in neutrophils, reduces neutrophil chemotaxis and protects the organism from both sterile and non-sterile inflammatory assaults (Hsu et al., 2017). A hematopoietic specific isoform of the small GTPase, *rac2,* was identified as a direct target of *miR-722.* Here, we used the tet-on technique to induce the overexpression of *miR-722* in differentiated HL-60 cells and uncovered a similar suppressive function of *miR-722* in human neutrophils.

2. Material and Methods

2.1. Generation of stable HL-60 cell lines

HEK-293 cells were cultured in DMEM supplemented with 10% FBS, 4.5 g/glucose and sodium bicarbonate. HL-60 cells were obtained from ATCC (CCL-240) and cultured using RPMI-1640 with HEPEs supplemented with 10% FBS with sodium bicarbonate. The lentiviral backbone pLIX_403 was a gift from David Root (Addgene plasmid # 41395). DNA sequence encoding microRNA-722 tagged with Dendra2 were amplified from (Addgene plasmid # 97163) with the following primers: pLIX-mir+: 5'-TGGAGAATTGGCTAGCGCCACCATGGATGAGGAAA TCGC-3', pLIX-mir-: 5'-CATACGGATAACCGGTTACCACACCTGGCTGGGC-3'and cloned into pLIX_403 vector using the NheI/AgeI sites. Stable HL-60 cell lines were generated as described (Cavnar et al., 2011). Briefly, HEK-293 cells were transfected with pLIX_403, VSV-G and CMV8.2 using lipofectamine 3000 (ThermoFisher). The viral supernatant was harvested on day three and concentrated with Lenti-X concentrator (Clontech). HL-60 Cells were spin infected at 2000 g for two hours at 32 °C and then selected and maintained in medium supplemented with 1 μg/ml puromycin. Live cells that excluded trypan blue stained cells were counted using a hemocytometer.

2.2. Epifluorescence microscope imaging

Induction of the Dendra2 reporter expression was verified by imaging the green fluorescence using AXIO Zoom V16 microscope (Zeiss) at 110 % magnification. All images were acquired under the same condition within the linear range of the CCD detector. Dendra2+ Cell quantification was done by image J by measuring the mean fluorescence intensity of the dendra2 channel and divided by DAPI based cell count.

2.3. RT-qPCR

Total RNA was purified using MiRVANA miRNA purification kit (ThermoFisher). MicroRNAs were reverse transcribed with Universal cDNA Synthesis Kit II (Exiqon). MicroRNA RT-qPCR was performed with ExiLENT SYBR® Green master mix (Exiqon) using LightCycler ® 96 Real-Time PCR System (Roche Life Science). Primers used in this study are: miR-223–3p (205986), dre-miR-722 (2107521), hsa-let-7e-5p (205711) and human U6 (203907). Messenger RNAs were reverse transcribed with Transcriptor First Strand cDNA Synthesis Kit (Roche). RT-qPCR were performed with FastStart Essential DNA Green Master (Roche). Primers used are: pre722+: 5'-cggagtggaatttgaaacgttttggc-3'; pre722-:5'-cggagcgaaatctgaaacgtttctgc-3'; CCL2+: 5'-agtctctgccgcccttct-3'; CCL2-: 5'-gtgactggggcattgattg-3'; CLEC4A+: 5'-cccctcttgaggatatgtgc-3'; CLEC4A-: 5'-aggaaccaaacatggtggtaa-3'; C5AR1+: 5'-aagtaatgatacagagggatcttgtg-3'; C5AR1-: 5'-ttgcaagatgttgccattg-3'; CR1+: 5'-ctccccctcggtgtatttct-3'; CR1-: 5'-cctgtttcctggtactctaattgc-3'; FPR1+: 5'-tctctgctggtccccatatc-3'; FPR1-: 5'-ttgcaataactcacggattctg-3'; RAC2+: 5'-gatgcaggccatcaagtgt-3'; RAC2-: 5'-ctgatgagaaggcaggtcttg-3'; GAPDH+: 5'-ccccggtttctataaattgagc-3'; GAPDH-: 5'-cttccccatggtgtctgag-3'. The specificity of the primers were verified with a single peak in the melt-curve. The relative fold change with correction of the primer efficiencies was calculated following instructions provided by Real-time PCR Minor (http://ewindup.info/miner/datasubmit.htm) and normalized to *U6* (miRNA) and *GAPDH* (mRNA) respectively.

2.4. Flow Cytometry

Cells were stained with Alexa Fluor 647 conjugated CD11b (neutrophil differentiation marker, Biolegend, 301319, clone IV-M047) or the isotype control antibody (Biolegend, 400130, clone MOPC-21) and RUO AnnexinV (apoptosis marker, BD, 563973). Cells were stained in staining buffer (1%BSA 0.1% NaN_3) and incubated on ice for 1 hour, washed three times with staining buffer and resuspended to suitable volume. Dendra 2 reporter expression levels were collected with the 488nM excitation filter and 530/30 PMT. Fluorescence intensity and collected using BD LSR Fortessa. Results were analyzed with Beckman Kaluza 2.1 software.

2.5. RNAseq

HL-60 cells were differentiated for 4 days in 1.3% DMSO (Jacob et al., 2002), induced with 1μg/ml doxycycline or left un-induced for 2 additional days, and then pelleted into microtubes each containing 107 cells. Total mRNA was extracted using RNeasy Plus Mini Kit (Qiagen #74104). RNAseq was performed at The Center for Medical Genomics at Indiana University School of Medicine. Samples were polyA enriched and sequenced with Illumina HiSeq 4000 with reads range from 37M to 44M. The RNA-seq raw data and processed data are in the process of being submitted to the Gene Expression Omnibus (GEO) and will be publicly available upon the acceptance of the manuscript.

2.6. Bioinformatics analysis on RNA-seq data

The sequencing reads was mapped to the human genome using STAR v2.5 RNA-seq aligner (Dobin et al., 2013) with the following parameter: "--outSAMmapqUnique 60". Uniquely

mapped sequencing reads were assigned to hg38 genes using featureCounts v1.6.2 (Liao et al., 2014) with the following parameters: "-s 2 –p –Q 10". The genes were filtered if their count per million of reads were less than 0.5 in more than 4 of the samples. The trimmed mean of M values method was used for normalization on gene expression profile across all samples, followed by the differential expression analysis using edgeR v3.20.8 (McCarthy et al., 2012; Robinson et al., 2010). The gene was determined as differentially expressed gene if its p-value after FDR-adjusted multiple-test correction was less than 0.01 and its amplitude of fold change was larger than 1.8. We identified 1943 down-regulated DEGs and 632 up-regulated DEGs by comparing miR-722 ± Dox. However, no DEG was recognized for the control line based on the same cutoffs. The software package, DAVID Bioinformatics Resources 6.8 (Huang da et al., 2009a, b) was adopted for Gene Ontology and KEGG pathway enrichment analysis. The significant enriched GO terms or KEGG pathways were selected if their FDR-adjusted p-values (q-values) were less than 0.05 after multiple test correction, when we compared DEGs down-regulated by *miR-722* +Dox with all expressed genes tested by RNA-seq.

2.7. Innminoblotting

HL-60 cells were differentiated for 4 days in 1.3% DMSO (Jacob et al., 2002), induced with 1ug/ml Doxycycline or left un-induced for 2 additional days, and then pelleted into microtubes each containing 10^6 cells. Cells were lysed with RIPA buffer (Thermo #89900) supplemented with proteinase inhibitor cocktail (Roche # 4693132001). Protein content in the supernatant was determined with BCA assay (Thermo #23225) and 25~50 μg of protein were subjected to SDS-PAGE and transferred to nitrocellulose membrane. Immunoblotting was performed with a mice anti-RAC2 antibody (Millipore 07–604-I), a rabbit anti-Vinculin antibody (Sigma V9131) and goat anti-mouse (Invitrogen 35518) or anti-rabbit (Thermo SA5–35571) secondary antibodies. The fluorescence intensity was measured using an Odyssey imaging system (LI-COR).

2.8. Reporter assay

miR-722 or vector control constructs were cloned into PCDNA3.1 as described (Hsu et al., 2017). Human *RAC2* 3'UTR was amplified with One Step Ahead RT-PCR kit (Qiagen) from human mRNA using the following primers *RAC2* 3'UTR+: 5'-TAGGCGATCGCTCGAGGGGTTGCACCCCAGCGCT-3', *RAC2* 3'UTR- : 5'-TTGCGGCCAGCGGCCGCTCTCCAAACTTGAATCAATAAATTT-3' and inserted into a dual luciferase psiCHECK2 backbone (Promega). *RAC2* mutant 3'UTR constructs were generated using Infusion HD cloning kit (Clontech) with the following primers: *RAC2* mut +: 5'-GAGTTCCTCTACCCACGTTTTTTGAGTGTCTCAGAAGTGTGC-3', *RAC2* mut–: 5'-TGGGTAGAGGAACTCTCTGG-3. Mutation was confirmed with Sanger sequencing. HEK-293T cells seeded at 2×10^5/well in 12 well plates and transfected with the indicated *miR-722* overexpression and the RAC2 3'UTR reporter plasmids with Lipofectamine 3000 (Invitrogen). Cells were harvested and lysed at 48 h post transfection and luciferase activity was measured with Dual Glo-Luciferase reagent (Promega, PF-E2920) in a Synergy 2 (Biotek) plate reader. The renilla luciferase activity was normalized to the firefly luciferase, which was then normalized to the vector control.

2.9. Transwell migration assay

HL-60 transwell assays were performed as described (Cavnar et al., 2011). Briefly, differentiated cells were resuspended in HBSS buffer and allowed to migration for 2 h towards fMLP (100 nM). Cells that migrated to the lower chamber were released with 0.5M EDTA and counted using a BD LSRFortessa flow cytometer with an acquisition time of 30 sec. The counts were normalized with the total numbers of cells added to each well the data was then gated for live cells and analyzed with Beckman Kaluza 2.1 software.

2.10. 2D Chemotaxis assay

Differentiated HL-60 cells were resuspended in HBSS with 20mM HEPES and 0.5% FBS and loaded in collagen-coated IBIDI chemotaxis μ-slides (ibidi # 80326) and incubated at 37°C for 30 minutes to allow cells to adhere. 15 ul of 1000 nM fMLP was loaded into the right reservoir yielding a final fMLP concentration of 187 nM. Cell migration was recorded every 60 sec for 120 minutes using LSM 710 (with Ziess EC Plan-NEOFLUAR 10X/0.3 objective) at 37°C. Cells expressing Dendra2 with initial position on the left half of the channel were tracked with ImageJ plug-in MTrackJ as previously described (Meijering et al., 2012). Velocity and chemotaxis index were quantified using the ibidi cell migration tool.

2.11. Fluorescence microscopy

dHL-60 cells were resuspended in HBSS with 20 mM HEPES and 0.5% FBS and attached to fibrinogen-coated slides for 30 min at 37°C. Cells were then stimulated with 100 nM fMLP for 3 min at 37°C and fixed with 4% paraformaldehyde in PBS for 15 min at 37°C. The staining of fixed cells were performed as previously described (Fayngerts et al., 2017). Cells were permeabilized with 0.1% Triton X-100 and 3% BSA in PBS for 1 h at room temperature and blocked with 3% BSA in PBS for 1 h at room temperature. dHL-60 cells were incubated with phalloidin -AlexaFluor 568 (Invitrogen A12380) diluted 1:100 in 3% BSA overnight at 4°C. The cells were then stained with 1μg/ml DAPI (Invitrogen D3571) in 3% BSA for 1 h at room temperature. Images were acquired using a laser scanning confocal microscope LSM 710 (Zeiss) with a Plan-Apochromat 63x/1.4 Oil M27 or Plan-NEOFLUAR 10X/0.3 objective and processed with ImageJ.

2.12. ROS measurement

dHL-60s were treated with PMA 0.5 ng/μl or 100 nM fMLP and hydrogen peroxide levels in the culture media were measured using the Amplex® Red Hydrogen Peroxide/Peroxidase Assay Kit (Invitrogen A22188). Results were obtained using a Flexstation Multi-Mode Microplate Reader (Molecular Devices) with 544nM monochrome excitation and 590 emission bandpass filter. Background was normalized by subtracting the reading from samples treated with the vehicle control (DMSO for fMLP and ethanol for PMA respectively). Concentrations were calculated using a hydrogen peroxide standard curve.

2.13. Statistical Analysis

Statistical analysis was carried out using PRISM 6 (GraphPad). Mann–Whitney test (comparing two groups) and Kruskal–Wallis test (when comparing to single group) were used in this study as indicated in the figure legends. A representative experiment of at least

three independent repeats were shown. For qPCR, each gene was normalized to the reference gene and compared with Mann–Whitney tests. The statistical significance of overlap between miR-722 down-/up-regulated genes and miR-722 target genes was calculated using hypergeometric distribution.

3. Results

3.1. Establishing an inducible gene expression system in HL-60

To establish a platform that allows inducible gene expression in HL-60 cells, a lentiviral backbone initially constructed by Dr. David Root (Addgene plasmid # 41395) was selected. It contains all elements to enhance viral production and integration, including a Psi packaging element to facilitate pseudovirus production, REE and WPRE nuclear exporting elements to enhance integration in the host genome. The puromycin resistant gene and the reverse tetracycline-controlled transactivator is constantly expressed under the control of the PGK promoter. Addition of tetracycline or its close derivative doxycycline induces the binding of the transactivator to the tet responsive element, activating the target gene expression in a dose dependent manner (Figure 1A). The microRNA hairpin is cloned into the intron of a fluorescent reporter gene, *Dendra2.* To ensure an effective selection of cells with integration, we measured cell proliferation in the presence of increased doses of puromycin. HL-60 cells treated with 0.5 μg/ml puromycin continued to proliferate for one day before getting killed. Cells treated with 1 or 2 μg/ml puromycin were killed within the first day and continued to die out (Figure 1B). Based on this result, we selected the condition of 1 μg/ml puromycin treatment for at least 7 days to ensure the removal of untransduced cells. We then determined the dose of doxycycline differentiated HL-60 cells (dHL-60) can tolerate. Cells at 4 days post-differentiation were treated with increased doses of doxycycline, and cytotoxicity was observed at 3 and 5 μg/ml concentrations, but not at 1 μg/ml (Figure 1C), suggesting that doxycycline at 1 μg/ml is tolerated by dHL-60 cells.

3.2. Inducible expression of *miR-722* in HL-60

We then generated stable HL-60 lines in which the *miR-722* or a vector control expression is regulated by the tet responsive element. For simplicity, we refer to them as *miR-722* and control lines. After induction, we observed significant increases of the Dendra2 reporter expression with or without DMSO induced differentiation (Figure 1D, E). The experimental flow thus is finalized as depicted in Figure 2A. To confirm that *miR-722* expression is indeed induced, we quantified the levels of the precursor transcript and the mature microRNA. Since *miR-722* is absent in human and HL-60 cells, we detected 10,000 fold increase of the mature *miR-722* level in the *miR-722* line, but not in the control line (Figure 2B). The majority of the cells from both lines expressed a detectable level of the Dendra2 reporter (Figure 2C). General microRNA biogenesis was not affected, since the level of two other mature microRNA, *MIR-223* and *LET7* in dHL-60 was not affected. Additionally, cell viability or differentiation (as measured by surface expression of annexin V binding and CD11b expression) was not affected by overexpression of *miR-722* in dHL-60 cells (Figure 2D, E).

3.3. *miR-722* suppresses cell migration and signaling related genes in HL-60

To characterize the signaling pathways that are regulated by *miR-722,* we performed RNAseq of the *miR-722* and the control lines. Since lentiviral mediated DNA integration is random, although with some preferences (Deichmann et al., 2007; Felice et al., 2009), we compared the gene expression changes in both lines ± Dox to minimize the artifact associated with insertion sites. Induction of *miR-722* in dHL-60 resulted in significant dis-regulation of transcripts (FDR-adjusted p-value < 0.01 & FC < $-\log_2$l.8, see Methods for details) as shown in Figure 3A and Supplementary Dataset 1. There were more down-regulated differentially expressed genes (DEGs) (n = 1943) identified than up-regulated ones (n = 632), which is consistent with the function of microRNAs as suppressors of gene expression. Among the down-regulated transcripts, the human orthologues of predicted *miR-722* targets in zebrafish were significantly enriched (p = 0.003) (Figure 3B), while *miR-722* targets were depleted in up-regulated gene group (p = 0.031). The results indicate an evolutionary conservation of *miR-722* targets. Under the same cutoffs used in comparison in the *miR-722* line, no significant dysregulation was identified in the control line ± Dox, where only 15 transcripts had p < 0.01 without multiple-test correction (Supplementary Figure 1 and Supplementary Dataset 2). Moreover, fold changes of genes in the control line were presented in a symmetric way between up- and down-regulation. The different patterns between *miR-722* and vector suggests that the effect of *miR-722* was not due to the reporter gene expression alone. Via enrichment analysis on Gene Ontology and KEGG pathways, we found that the down regulated transcripts were significantly over-represented in pathways regulating cell migration, chemotaxis, signaling and inflammation (Figure 3C, D, E, F and Supplementary Dataset 3). To validate the RNAseq results, we quantified the relative expression level of several transcripts in the chemotaxis pathway and indeed all were significantly downregulated upon the induction of *miR-722,* but not the reporter gene alone (Figure 4A). Among the selected genes, the chemokine receptor encoding gene, *Fpr1,* harbors *miR-722* binding sites in its 3′UTR and is a potential direct target. Since *rac2* is a direct target of *miR-722* in zebrafish, we tested whether human *RAC2* is also a *miR-722* target. We detected significant down regulation of *RAC2* at both the transcript and protein levels upon *miR-722* overexpression (Figure 4A, B). Indeed, a 7mer-m8 site (complementarity at nt 2–7 and mismatch at nt8) was present in the *RAC2* 3′UTR (Figure 4C). In a luciferase reporter assay, specific suppression by *miR-722* was observed with the wild-type *RAC2* 3 ‘UTR, but not the mutated 3′UTR lacking the seed binding site (Figure 4D, E), confirming that *RAC2* is a direct target of *miR-722* in human cells.

3.4. *miR-722* suppresses chemotaxis and generation of reactive oxygen species in HL-60

RAC2 is essential for actin polymerization and migration in neutrophils (Carstanjen et al., 2005). The chemoattractant N-Formylmethionine-leucyl-phenylalanine (fMLP) induces rapid neutrophil polarization with lamellipodia in the front and a tail in the back (Srinivasan et al., 2003). In dHL-60 cells overexpressing *miR-722,* the formation of the lamellipodia and the establishment of polarity were significantly inhibited (Figure 5A, B). We then measured chemotaxis of the *miR-722* line using two independent assays. Cells were allowed to migrate towards fMLP in a chemotaxis slide. *miR-722* overexpressing cells displayed a significant defect in velocity but not in directionality, compared with the vector control or the *miR-722* expressing line without doxycycline mediated induction (Figure 5C–E,

Supplementary Movie 1, 2). Consistently, *miR-722* overexpression suppressed cell transwell migration (Figure 5F). In addition to the regulation of the cytoskeleton, RAC2 also regulates the activation of the NADPH oxidase and thus the generation of reactive oxygen species (ROS) in human neutrophils (Dusi et al., 1996). Upon *miR-722* overexpression, the dHL-60 cells secreted significantly reduced amounts of hydrogen peroxide in the culture media when stimulated with phorbol 12-myristate 13-acetate or fMLP (Figure 6). The reduced chemotaxis and generation of ROS are consistent with a reduced RAC2 level in the cells, although it is possible that the downregulation of other *miR-722* targets also contributes to these phenotypes.

4. Discussion

Here we have applied the tet-on system in differentiated HL-60 (dHL-60) cells and uncovered an evolutionally conserved role of *miR-722* in suppressing neutrophil migration and signaling.

To our knowledge, it is the first application of the tet-on system in dHL-60 cells. Tet-on and tet-off system is favored in biomedical research because acute depletion or overexpression is more faithfully in reflecting the target gene function. The caveat of chronic depletion or overexpression is the possible compensatory expression of other off-target genes and altered overall cell physiology, which will complicate the result interpretation. An additional challenge with using dHL-60 cell model to study neutrophil function is the required differentiation process. It is essentially impossible to study genes that would affect cell differentiation without an inducible system. The dose of doxycycline dHL-60 could tolerate (1 μg/ml) is significantly lower than that in other cell lines (10 μg/ml). Although doxycycline is a broad spectrum antibiotic that inhibit bacterial protein synthesis, it also inhibits protein synthesis in eukaryotic mitochondria and thus can impair cell metabolism and cause cell death (Chatzispyrou et al., 2015; Moullan et al., 2015). The mechanism underlying this increased sensitivity is not clear but could be due to increased uptake and/or decreased efflux of doxycycline in dHL-60. In addition, doxycycline or its degradation products may be highly toxic to dHL-60s. We have optimized our protocol where the cytotoxicity of doxycycline is not observed. Cell proliferation, survival and differentiation were not affected by doxycycline treatment. We expect that our method is equally applicable to the inducible expression of other RNA species such as shRNAs in dHL-60, providing a platform for acute depletion of endogenous proteins to evaluate their biological significance in mature cell function without affecting the differentiation process.

Fundamental biological processes, such as cell proliferation and migration, are conserved through evolution. It is estimated that ~60 % of human protein-coding genes are under selective pressure to maintain miRNA seed binding sites in the 3′UTR which are conserved in vertebrates (Friedman et al., 2009). Data compiled from previous microRNA sequencing experiments suggest that *miR-722* is intergenic and predominantly produce a mature 3p strand that harbors binding sequences of specific genes, e.g. *Rac2* (www.miRbase.org). It is not surprising that both human *RAC2* and zebrafish *Rac2* are direct *miR-722* targets. It is intriguing that *miR-722* expression in human HL-60 cells resulted in a down-regulation of genes that are significantly enriched for the orthologues of the predicted zebrafish targets.

The significantly altered pathways provides explanation of the anti-inflammatory effect of this microRNA in zebrafish as its overexpression protected zebrafish against lethal inflammatory assault (Hsu et al., 2017).

Rac2 plays a principal role in regulating the actin cytoskeleton, chemotaxis and signaling. Rac2 is required for neutrophil motility and chemotaxis (Yoo et al., 2010), retention in the hematopoietic tissue (Deng et al., 2011), generation of super oxide ions during infections (Jonzon and Bindslev, 1991) and degranulation of primary granules (Abdel-Latif et al., 2004). The therapeutic potential of Rac2 suppression in controlling inflammation has not been explored. Currently, a Rac2 specific inhibitor is not available and a complete Rac2 inhibition would result in primary immune deficiency and poor wound healing (Williams et al., 2000). Although the therapeutic potential of *miR-722* is not clear without further characterization, our work here has characterized the first microRNA that targets human *RAC2* and established *miR-722* as a suppressor for neutrophil migration and signaling.

The *miR-722* is not detected in human until now, suggesting that *miR-722* itself might not be evolutionarily conserved between zebrafish and human. The *miR-129–5p* share the same seed sequence (positions 2–8 of the mature miRNA) with *miR-722* (with a predominant 3p strand). The *miR-129* gene in human however produces both the 5p and 3p strand product. It is likely that *miR-129* targets additional sets of genes with two functional microRNA strands. We used bioinformatics to generate the list of predicted human targets of *miR-129–5p* and human orthologous genes of predicted *miR-722* targets in zebrafish. No enrichment of the predicted human *miR-129–5p* targets was observed in the *miR-722* down-regulated genes (Figure 3A), suggesting that *miR-722* mediated gene suppression is not completely dependent on seed matching. Alternatively, the indirect targets of *miR-722* are dominant in the downregulated gene list. Interestingly, the human orthologues of *miR-722* targets are significantly enriched in the *miR-722* downregulated gene list (Figure 3B). In addition, the human orthologues of *miR-722* targets are over-represented in the predicted *miR-129–5p* targets ($p = 0.017$), suggesting an evolutionary conservation of the *miR-722* binding sites.

In conclusion, we reported for the first time the method for inducible expression of microRNAs in HL-60s, which allows studying mature cell function without interfering with cell differentiation. Additionally, we provide evidence that zebrafish *miR-722* can suppress human RAC2 gene and cell migration. Nevertheless, further research is still needed to evaluate the therapeutic potential of this microRNA in inflammatory ailments.

Supplementary Material

Refer to Web version on PubMed Central for supplementary material.

Acknowledgement

The authors would like to thank Dr. Daoguo Zhou (Purdue University) for providing the Odyssey imaging system (LI-COR) and Dr. John Tesmer (Purdue University) for providing the Flexstation Multi-Mode Microplate Reader (Molecular Devices).

Funding: The work was supported by National Institutes of Health [R35GM119787 to DQ] and [P30CA023168 to Purdue Center for Cancer Research] for shared resources. Bioinformatics analysis was conducted by the Collaborative Core for Cancer Bioinformatics (C^3B) shared by the Indiana University Simon Cancer Center

[P30CA082709] and the Purdue University Center for Cancer Research with support from the Walther Cancer Foundation. AYH is supported by Purdue Research Foundation.

Abbreviations

tet-on	gene expression activated by doxycycline
Rac2	Ras-Related C3 Botulinum Toxin Substrate 2
miR	microRNA
DEG	differentially expressed gene
q-values	FDR-adjusted p-values
dHL-60	differentiated HL-60 cells (dHL-60)
FC	fold change
fMLP	N-Formylmethionine-leucyl-phenylalanine
ROS	reactive oxygen species

References

Abdel-Latif D, Steward M, Macdonald DL, Francis GA, Dinauer MC, Lacy P, 2004 Rac2 is critical for neutrophil primary granule exocytosis. Blood 104, 832–839. [PubMed: 15073033]

Abi Abdallah DS, Egan CE, Butcher BA, Denkers EY, 2011 Mouse neutrophils are professional antigen-presenting cells programmed to instruct Th1 and Th17 T-cell differentiation. International immunology 23, 317–326. [PubMed: 21422151]

Borregaard N, 2010 Neutrophils, from marrow to microbes. Immunity 33, 657–670. [PubMed: 21094463]

Bousquet M, Quelen C, Rosati R, Mansat-De Mas V, La Starza R, Bastard C, Lippert E, Talmant P, Lafage-Pochitaloff M, Leroux D, Gervais C, Viguie F, Lai JL, Terre C, Beverlo B, Sambani C, Hagemeijer A, Marynen P, Delsol G, Dastugue N, Mecucci C, Brousset P, 2008 Myeloid cell differentiation arrest by miR-125b-1 in myelodysplastic syndrome and acute myeloid leukemia with the t(2;11)(p21;q23) translocation. The Journal of experimental medicine 205, 2499–2506. [PubMed: 18936236]

Cao MW, Shikama Y, Kimura H, Noji H, Ikeda K, Ono T, Ogawa K, Takeishi Y, Kimura J, 2017 Mechanisms of Impaired Neutrophil Migration by MicroRNAs in Myelodysplastic Syndromes. Journal of immunology 198, 1887–1899.

Carstanjen D, Yamauchi A, Koornneef A, Zang H, Filippi MD, Harris C, Towe J, Atkinson S, Zheng Y, Dinauer MC, Williams DA, 2005 Rac2 regulates neutrophil chemotaxis, superoxide production, and myeloid colony formation through multiple distinct effector pathways. Journal of immunology 174, 4613–4620.

Cavnar PJ, Berthier E, Beebe DJ, Huttenlocher A, 2011 Hax1 regulates neutrophil adhesion and motility through RhoA. The Journal of cell biology 193, 465–473. [PubMed: 21518791]

Chatzispyrou IA, Held NM, Mouchiroud L, Auwerx J, Houtkooper RH, 2015 Tetracycline Antibiotics Impair Mitochondrial Function and Its Experimental Use Confounds Research. Cancer research 75, 4446–4449. [PubMed: 26475870]

Chen H, Chen Q, Fang M, Mi Y, 2010 microRNA-181b targets MLK2 in HL-60 cells. Sci China Life Sci 53, 101–106. [PubMed: 20596961]

Deichmann A, Hacein-Bey-Abina S, Schmidt M, Garrigue A, Brugman MH, Hu J, Glimm H, Gyapay G, Prum B, Fraser CC, Fischer N, Schwarzwaelder K, Siegler ML, de Ridder D, Pike-Overzet K, Howe SJ, Thrasher AJ, Wagemaker G, Abel U, Staal FJT, Delabesse E, Villeval JL, Aronow B,

Hue C, Prinz C, Wissler M, Klanke C, Weissenbach J, Alexander I, Fischer A, von Kalle C, Cavazzana-Calvo M, 2007 Vector integration is nonrandom and clustered and influences the fate of lymphopoiesis in SCID-X1 gene therapy. Journal of Clinical Investigation 117, 2225–2232. [PubMed: 17671652]

Deng Q, Yoo SK, Cavnar PJ, Green JM, Huttenlocher A, 2011 Dual roles for Rac2 in neutrophil motility and active retention in zebrafish hematopoietic tissue. Developmental cell 21, 735–745. [PubMed: 22014524]

Dobin A, Davis CA, Schlesinger F, Drenkow J, Zaleski C, Jha S, Batut P, Chaisson M, Gingeras TR, 2013 STAR: ultrafast universal RNA-seq aligner. Bioinformatics 29, 15–21. [PubMed: 23104886]

Dusi S, Donini M, Rossi F, 1996 Mechanisms of NADPH oxidase activation: translocation of p40phox, Rac1 and Rac2 from the cytosol to the membranes in human neutrophils lacking p47phox or p67phox. The Biochemical journal 314 (Pt 2), 409–412. [PubMed: 8670049]

Ergin K, Bozkurt G, Cubuk C, Aktas S, 2015 Effect of Resveratrol on microRNA Profile and Apoptosis in HL-60 Leukemia and Raji Lymphoma Cells. Meand Med Dent J 16, 83–90.

Fabian MR, Sonenberg N, 2012 The mechanics of miRNA-mediated gene silencing: a look under the hood of miRISC. Nature structural & molecular biology 19, 586–593.

Fayngerts SA, Wang Z, Zamani A, Sun H, Boggs AE, Porturas TP, Xie W, Lin M, Cathopoulis T, Goldsmith JR, Vourekas A, Chen YH, 2017 Direction of leukocyte polarization and migration by the phosphoinositide-transfer protein TIPE2. Nat Immunol 18, 1353–1360. [PubMed: 29058702]

Felice B, Cattoglio C, Cittaro D, Testa A, Miccio A, Ferrari G, Luzi L, Recchia A, Mavilio F, 2009 Transcription factor binding sites are genetic determinants of retroviral integration in the human genome. PloS one 4, e4571. [PubMed: 19238208]

Friedman RC, Farh KKH, Burge CB, Bartel DP, 2009 Most mammalian mRNAs are conserved targets of microRNAs. Genome research 19, 92–105. [PubMed: 18955434]

Gantier MP, 2013 The not-so-neutral role of microRNAs in neutrophil biology. Journal of leukocyte biology 94, 575–583. [PubMed: 23322875]

Gurol T, Zhou W, Deng Q, 2016 MicroRNAs in neutrophils: potential next generation therapeutics for inflammatory ailments. Immunological reviews 273, 29–47. [PubMed: 27558326]

Hsu AY, Wang D, Gurol T, zhou W, Zhu X, Lu HY, Deng Q, 2017 Overexpression of microRNA-722 fine-tunes neutrophilic inflammation by inhibiting Rac2 in zebrafish. Disease models & mechanisms 10, 1323–1332. [PubMed: 28954734]

Huang da W, Sherman BT, Lempicki RA, 2009a Bioinformatics enrichment tools: paths toward the comprehensive functional analysis of large gene lists. Nucleic acids research 37, 1–13. [PubMed: 19033363]

Huang da W, Sherman BT, Lempicki RA, 2009b Systematic and integrative analysis of large gene lists using DAVID bioinformatics resources. Nat Protoc 4, 44–57. [PubMed: 19131956]

Huang K, Dong B, Wang Y, Tian T, Zhang B, 2015 MicroRNA-519 enhances HL60 human acute myeloid leukemia cell line proliferation by reducing the expression level of RNA-binding protein human antigen R. Molecular medicine reports 12, 7830–7836. [PubMed: 26499919]

Jacob C, Leport M, Szilagyi C, Allen JM, Bertrand C, Lagente V, 2002 DMSO-treated HL60 cells: a model of neutrophil-like cells mainly expressing PDE4B subtype. International immunopharmacology 2, 1647–1656. [PubMed: 12469939]

Jian P, Li ZW, Fang TY, Jian W, Zhuan Z, Mei LX, Yan WS, Jian N, 2011 Retinoic acid induces HL-60 cell differentiation via the upregulation of miR-663. Journal of hematology & oncology 4, 20. [PubMed: 21518431]

Jonzon KH, Bindslev L, 1991 [Acute severe respiratory insufficiency in adults as a complication of septic and traumatic shock]. Lakartidningen 88, 4145–4148. [PubMed: 1956254]

Kasashima K, Nakamura Y, Kozu T, 2004 Altered expression profiles of microRNAs during TPA-induced differentiation of HL-60 cells. Biochemical and biophysical research communications 322, 403–410. [PubMed: 15325244]

Kawasaki H, Taira K, 2004 MicroRNA-196 inhibits HOXB8 expression in myeloid differentiation of HL60 cells. Nucleic acids symposium series, 211–212. [PubMed: 17150553]

Kolaczkowska E, Kubes P, 2013 Neutrophil recruitment and function in health and inflammation. Nature Reviews Immunology 13, 159–175.

Landgraf P, Rusu M, Sheridan R, Sewer A, Iovino N, Aravin A, Pfeffer S, Rice A, Kamphorst AO, Landthaler M, Lin C, Socci ND, Hermida L, Fulci V, Chiaretti S, Foa R, Schliwka J, Fuchs U, Novosel A, Muller RU, Schermer B, Bissels U, Inman J, Phan Q, Chien M, Weir DB, Choksi R, De Vita G, Frezzetti D, Trompeter HI, Hornung V, Teng G, Hartmann G, Palkovits M, Di Lauro R, Wernet P, Macino G, Rogler CE, Nagle JW, Ju J, Papavasiliou FN, Benzing T, Lichter P, Tam W, Brownstein MJ, Bosio A, Borkhardt A, Russo JJ, Sander C, Zavolan M, Tuschl T, 2007 A mammalian microRNA expression atlas based on small RNA library sequencing. Cell 129, 1401–1414. [PubMed: 17604727]

Lanotte M, Martin-Thouvenin V, Najman S, Balerini P, Valensi F, Berger R, 1991 NB4, a maturation inducible cell line with t(15;17) marker isolated from a human acute promyelocytic leukemia (M3). Blood 77, 1080–1086. [PubMed: 1995093]

Larsen MT, Hother C, Hager M, Pedersen CC, Theilgaard-Monch K, Borregaard N, Cowland JB, 2013 MicroRNA profiling in human neutrophils during bone marrow granulopoiesis and in vivo exudation. PloS one 8, e58454. [PubMed: 23554893]

Liamina D, Sibirnyj W, Khokhlova A, Saenko V, Rastorgueva E, Fomin A, Saenko Y, 2017 Radiation-Induced Changes of microRNA Expression Profiles in Radiosensitive and Radioresistant Leukemia Cell Lines with Different Levels of Chromosome Abnormalities. Cancers 9.

Liang H, Dong Z, Liu JF, Chuang W, Gao LZ, Ren YG, 2017 Targeting miR-155 suppresses proliferation and induces apoptosis of HL-60 cells by targeting Slug/PUMA signal. Histology and histopathology 32, 899–907. [PubMed: 27786352]

Liao Y, Smyth GK, Shi W, 2014 featureCounts: an efficient general purpose program for assigning sequence reads to genomic features. Bioinformatics 30, 923–930. [PubMed: 24227677]

Lim K, Hyun YM, Lambert-Emo K, Capece T, Bae S, Miller R, Topham DJ, Kim M, 2015 Neutrophil trails guide influenza-specific CD8(+) T cells in the airways. Science 349, aaa4352. [PubMed: 26339033]

Lin Y, Li D, Liang Q, Liu S, Zuo X, Li L, Sun X, Li W, Guo M, Huang Z, 2015 miR-638 regulates differentiation and proliferation in leukemic cells by targeting cyclin-dependent kinase 2. The Journal of biological chemistry 290, 1818–1828. [PubMed: 25451924]

McCarthy DJ, Chen Y, Smyth GK, 2012 Differential expression analysis of multifactor RNA-Seq experiments with respect to biological variation. Nucleic acids research 40, 4288–4297. [PubMed: 22287627]

Meijering E, Dzyubachyk O, Smal I, 2012 Methods for cell and particle tracking. Methods in enzymology 504, 183–200. [PubMed: 22264535]

Moullan N, Mouchiroud L, Wang X, Ryu D, Williams EG, Mottis A, Jovaisaite V, Frochaux MV, Quiros PM, Deplancke B, Houtkooper RH, Auwerx J, 2015 Tetracyclines Disturb Mitochondrial Function across Eukaryotic Models: A Call for Caution in Biomedical Research. Cell reports.

Nathan C, 2006 Neutrophils and immunity: challenges and opportunities. Nature reviews. Immunology 6, 173–182.

Pedruzzi E, Fay M, Elbim C, Gaudry M, Gougerot-Pocidalo MA, 2002 Differentiation of PLB-985 myeloid cells into mature neutrophils, shown by degranulation of terminally differentiated compartments in response to N-formyl peptide and priming of superoxide anion production by granulocyte-macrophage colony-stimulating factor. British journal of haematology 117, 719–726. [PubMed: 12028049]

Pizzimenti S, Ferracin M, Sabbioni S, Toaldo C, Pettazzoni P, Dianzani MU, Negrini M, Barrera G, 2009 MicroRNA expression changes during human leukemic HL-60 cell differentiation induced by 4-hydroxynonenal, a product of lipid peroxidation. Free radical biology & medicine 46, 282–288. [PubMed: 19022373]

Robinson MD, McCarthy DJ, Smyth GK, 2010 edgeR: a Bioconductor package for differential expression analysis of digital gene expression data. Bioinformatics 26, 139–140. [PubMed: 19910308]

Sharifi M, Salehi R, Gheisari Y, Kazemi M, 2014 Inhibition of microRNA miR-92a induces apoptosis and necrosis in human acute promyelocytic leukemia. Advanced biomedical research 3, 61. [PubMed: 24627869]

Shen C, Chen MT, Zhang XH, Yin XL, Ning HM, Su R, Lin HS, Song L, Wang F, Ma YN, Zhao HL, Yu J, Zhang JW, 2016 The PU.1-Modulated MicroRNA-22 Is a Regulator of Monocyte/Macrophage Differentiation and Acute Myeloid Leukemia. PLoS genetics 12.

Soehnlein O, Steffens S, Hidalgo A, Weber C, 2017 Neutrophils as protagonists and targets in chronic inflammation. Nature Reviews Immunology 17, 248–261.

Sreeramkumar V, Adrover JM, Ballesteros I, Cuartero MI, Rossaint J, Bilbao I, Nacher M, Pitaval C, Radovanovic I, Fukui Y, McEver RP, Filippi MD, Lizasoain I, Ruiz-Cabello J, Zarbock A, Moro MA, Hidalgo A, 2014 Neutrophils scan for activated platelets to initiate inflammation. Science 346, 1234–1238. [PubMed: 25477463]

Srinivasan S, Wang F, Glavas S, Ott A, Hofmann F, Aktories K, Kalman D, Bourne HR, 2003 Rac and Cdc42 play distinct roles in regulating PI(3,4,5)P3 and polarity during neutrophil chemotaxis. The Journal of cell biology 160, 375–385. [PubMed: 12551955]

Wang SL, Lv JF, Cai YH, 2016 Targeting miR-9 suppresses proliferation and induces apoptosis of HL-60 cells by PUMA upregulation in vitro. Int J Clin Exp Med 9, 19581–19587.

Wang XS, Gong JN, Yu J, Wang F, Zhang XH, Yin XL, Tan ZQ, Luo ZM, Yang GH, Shen C, Zhang JW, 2012 MicroRNA-29a and microRNA-142–3p are regulators of myeloid differentiation and acute myeloid leukemia. Blood 119, 4992–5004. [PubMed: 22493297]

Ward JR, Heath PR, Catto JW, Whyte MK, Milo M, Renshaw SA, 2011 Regulation of neutrophil senescence by microRNAs. PloS one 6, e15810. [PubMed: 21283524]

Warnatsch A, Ioannou M, Wang Q, Papayannopoulos V, 2015 Neutrophil extracellular traps license macrophages for cytokine production in atherosclerosis. Science 349, 316–320. [PubMed: 26185250]

Williams DA, Tao W, Yang FC, Kim C, Gu Y, Mansfield P, Levine JE, Petryniak B, Derrow CW, Harris C, Jia BQ, Zheng Y, Ambruso DR, Lowe JB, Atkinson SJ, Dinauer MC, Boxer L, 2000 Dominant negative mutation of the hematopoietic-specific Rho GTPase, Rac2, is associated with a human phagocyte immunodeficiency. Blood 96, 1646–1654. [PubMed: 10961859]

Woodfin A, Voisin MB, Beyrau M, Colom B, Caille D, Diapouli FM, Nash GB, Chavakis T, Albelda SM, Rainger GE, Meda P, Imhof BA, Nourshargh S, 2011 The junctional adhesion molecule JAM-C regulates polarized transendothelial migration of neutrophils in vivo. Nat Immunol 12, 761–U145. [PubMed: 21706006]

Yoo SK, Deng Q, Cavnar PJ, Wu YI, Hahn KM, Huttenlocher A, 2010 Differential regulation of protrusion and polarity by PI3K during neutrophil motility in live zebrafish. Developmental cell 18, 226–236. [PubMed: 20159593]

Highlights

- Inducible co-expression of a protein coding gene and a microRNA in HL-60 cells.
- *dre-miR-722* over-expression suppresses signaling in differentiated HL-60 cells.
- *dre-miR-722* directly suppresses the expression of human *RAC2* gene.
- *dre-miR-722* suppresses chemotaxis and oxidative burst in HL-60 cells.

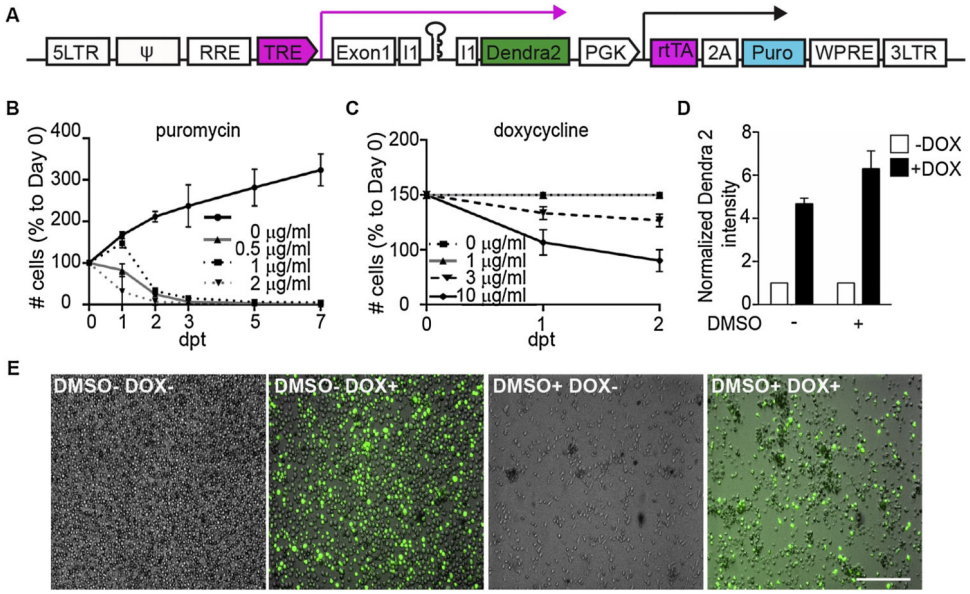

Figure 1. Inducible expression of a miRNA together with a reporter gene in HL-60 cells.

(A) Schematics of the plix 4.03 vector modified for the inducible expression of a microRNA and a reporter. The miRNA hairpin resides in the intron of the Dendra2 reporter (green) under the control of a doxycycline response element (TRE, magenta and magenta arrow). The puromycin resistant cassette (Puro, cyan) linked with the reverse tetracycline-controlled transactivator (rtTA, magenta) was driven by a constitutively active PGK promoter (black arrow). Flanking elements including the Psi packaging element, REE and WPRE nuclear exporting elements enhance integration in the host genome. (B) Proliferation of HL-60 cells in the presence of the indicated doses of puromycin. Cell numbers were normalized to day 0; dpt: days post treatment. (C) Survival of differentiated HL-60 cells in the presence of the indicated doses of doxycycline starting 4 day post differentiation. Cell numbers were normalized to day 0; dpt, days post treatment. (B, C) Results are averaged of three independent experiments and shown as mean ± s.d.. (D, E) Quantification (D) and representative images (E) of a stable line of HL-60 cells transduced with the construct depicted in (A) with/without differentiation (± DMSO) or induction (± DOX). Scale bar: 200 μm. (D) Mean fluorescence intensity was normalized with cell number and fold increase compared to uninduced controls are shown. Results are presented as mean ± s.d. from three independent experiments. **, $p < 0.01$, ****, $p < 0.0001$, Mann–Whitney test.

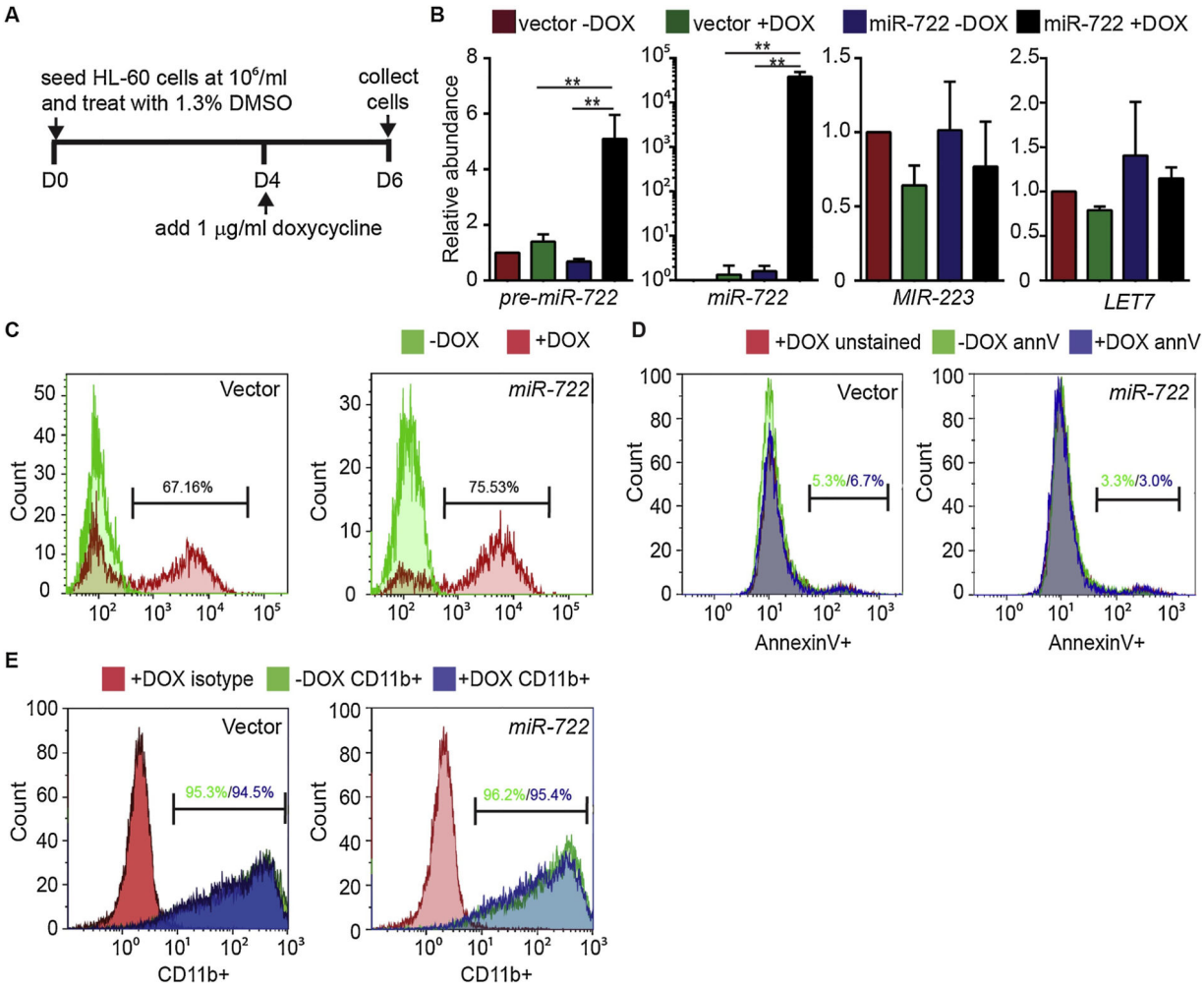

Figure 2. Specific induction of *miR-722* does not affect HL-60 differentiation or survival.

(A) Schematics of the experimental flow for the inducible expression of a microRNA and a reporter. The stable HL-60 cell lines over expressing *miR-722* or the vector control were differentiated with 1.3 % DMSO for 6 days and treated with 1 μg/ml doxycycline from day 4 or left untreated. (B) Levels of *pre-miR-722, miR-722, MIR-223,* and *LET7* in vector or miR-722 expressing dHL-60 lines ± doxycycline (DOX). Messenger RNAs were normalized to *GAPDH* and miRNAs were normalized to *U6.* Results are presented as mean ± s.d. from three independent experiments. **, $p < 0.01$, Mann–Whitney test. (C, D, E) Histogram of Dendra 2 expression (C), Annexin V staining (D), and CD11b expression (E) of vector and *miR-722* expressing dHL-60 with or without DOX. Positive cells are gated based on –DOX (C), unstained (D) or isotype control (E) and percentages of positive cells are labeled in corresponding color. Images are representative of three independent experiments.

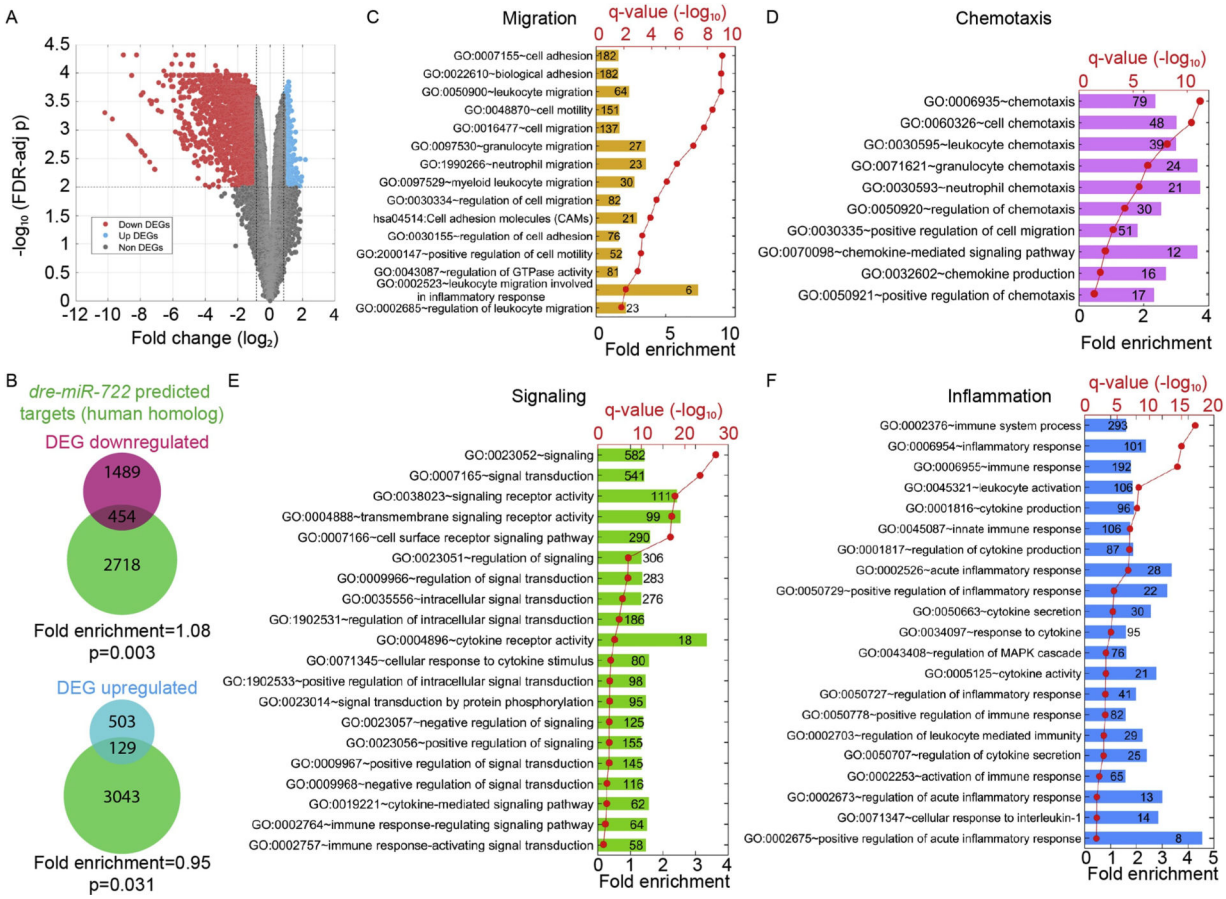

Figure 3. *miR-722* overexpression suppresses the expression of cell signaling and migration related genes in dHL-60.

(A) Volcano blot of DEGs with significant changes in expression upon doxycycline induced *miR-722* expression. Red: down-regulated differentially expressed genes (DEGs); cyan: up-regulated DEGs. (B) Significant enrichment of human homologues of *miR-722* predicted target genes in the down-regulated DEGs. $P < 0.003$, hypergeometric distribution. (C, D, E, F) Clusters of the genes in the pathways significantly altered upon *miR-722* overexpression. Number of the genes with significant expression changes in each pathway are labeled in each column. q-values, FDR-adjusted p-values as described in the Methods section.

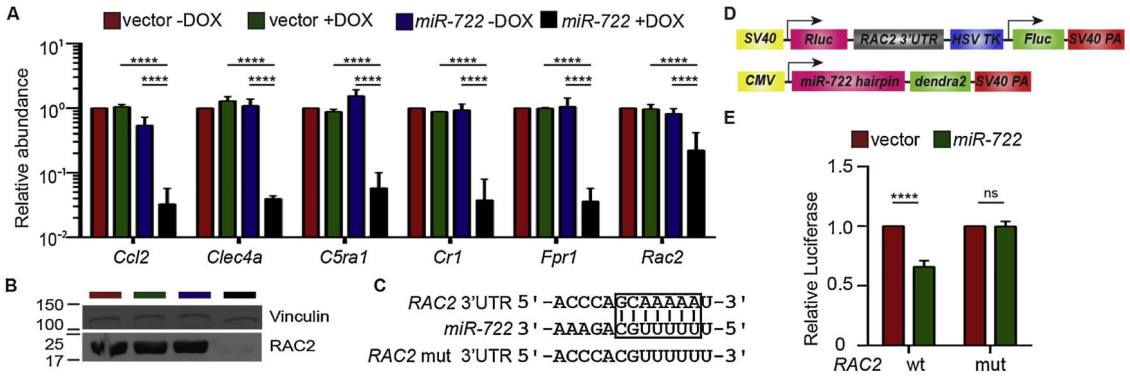

Figure 4. *RAC2* is a direct target of *miR-722*.

(A) Relative abundance of mRNA levels of indicated genes in vector or *miR-722* expressing dHL-60 ± DOX. Results are presented as mean ± s.d. from three independent experiments. ****, $p < 0.0001$, Sidak's multiple comparisons test. (B) Immunoblot of RAC2 in vector or *miR-722* expressing dHL-60 cells ± DOX. Vinculin is used as a loading control. The blot was cut in half and probed with two different primary antibodies. (C) Alignment of *miR-722* seed sequence and the 7mer-m8 seed binding site in the *RAC2* 3′UTR which is then mutated for the reporter assay in (E). (D) Schematics of the constructs used for the luciferase reporter assay. Wild-type or mutated *RAC2* 3′UTR were cloned downstream of a renilla luciferase gene. A firefly luciferase gene on the same plasmid was used as a normalization control. *mir-722* or vector hairpin was cloned into a mammalian expression plasmid for expression. (E) Selective suppression of renilla luciferase activity by *miR-722* through binding to the seed sequence in *RAC2* 3′UTR. Results are presented as means ± s.d. from three independent experiments. ****, $p < 0.0001$, Mann–Whitney test.

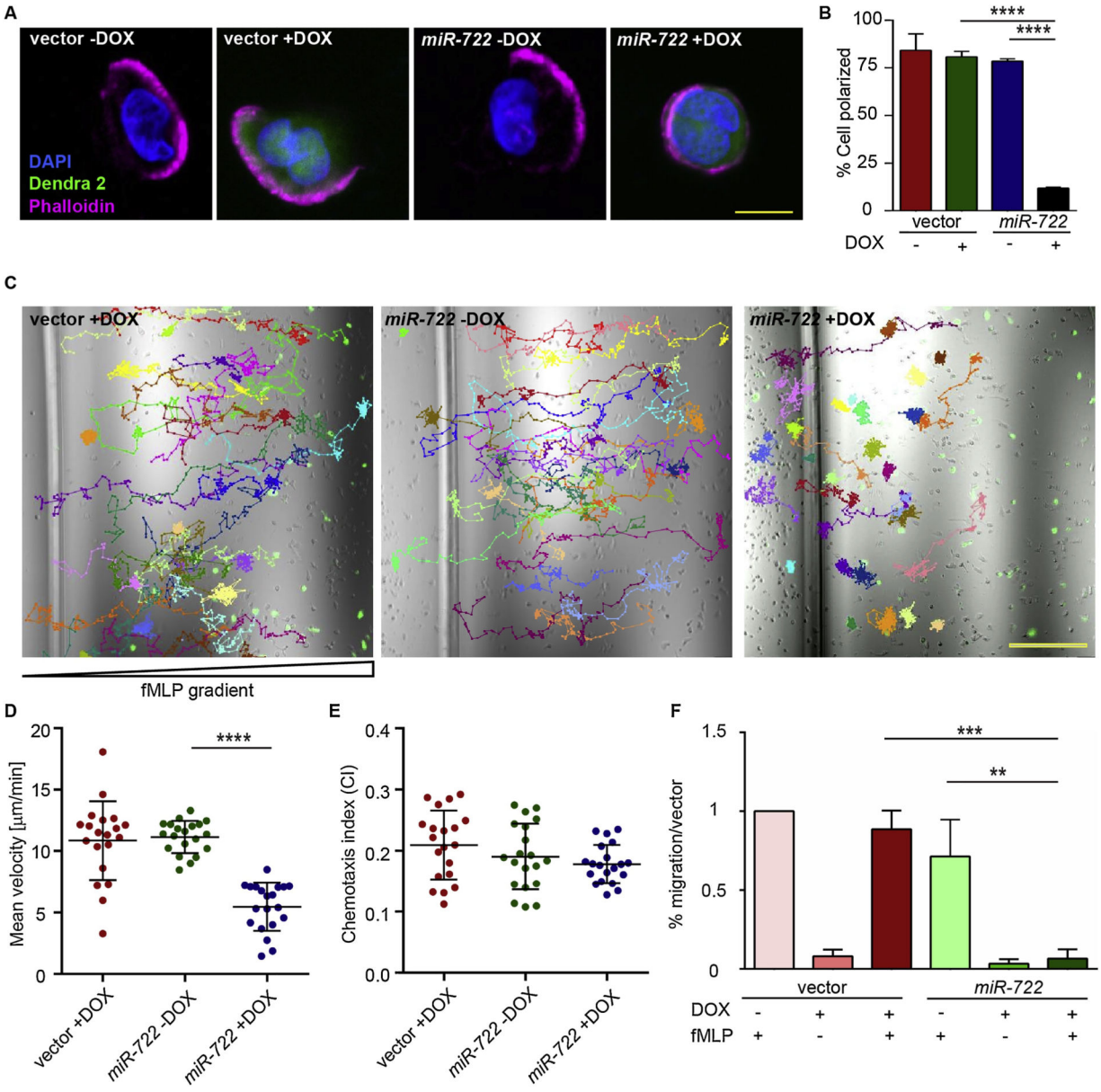

Figure 5. *MiR-722* overexpression suppresses dHL-60 chemotaxis.

(A, B) Representative fluorescence images (A) and quantification of polarized polymerization of acitn (B) of vector or *miR-722* expressing dHL-60 ± DOX after fMLP (100 nM) stimulation. Magenta, phalloidin; blue, DAPI; green: dendra2. Scale bar: 10 µm. (B) Results are presented as mean ± s.d. from three independent experiments. ****, p<0.0001, Sidak's multiple comparisons test. (C) Representative images and tracks of dHL-60 cells expressing either vector (left) or *miR-722* with (right) and without (middle) doxycycline toward fMLP. Scale bar: 200 µm. (D, E) Quantification of velocity (D) and directionality (E) of dHL-60 cells during 2D chemotaxis. Results are representative of three independent experiments. ****, p < 0.0001, Sidak's multiple comparisons test. (F) Transwell migration of vector or *miR-722* expressing dHL-60 cells towards fMLP. Results

are presented as mean ± s.d. from three independent experiments. **, $p < 0.01$; ***, $p<0.001$, Sidak's multiple comparisons test.

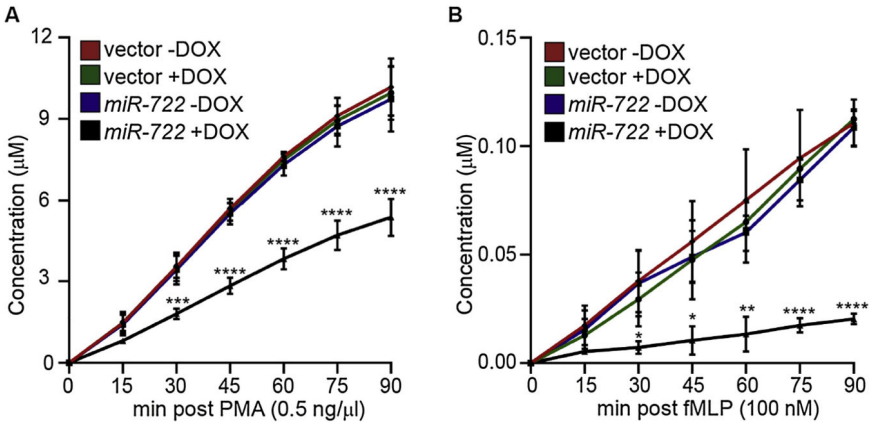

Figure 6. *MiR-722* overexpression suppresses ROS production in dHL-60.

(A and B) Secretion of hydrogen peroxide from vector or *miR-722* expressing dHL-60 stimulated with PMA (0.5 ng/ml) (A) or fMLP (100 nM) (B). Hydrogen peroxide levels were measured every 15 minutes for 90 minutes. Results are presented as mean ± s.d. of three independent experiments., *, $p<0.05$, **, $p < 0.01$; ***, $p<0.001$, ****, $p<0.0001$, Sidak's multiple comparisons test.